

Radiative cooling of shocked gas in stellar atmospheres

I. Contribution from spectral lines

A. Fokin¹, G. Massacrier², and D. Gillet³

¹ Institute of Astronomy of the Russian Academy of Sciences, 48 Pjatnitskaya Str., Moscow 109017, Russia (fokin@inasan.rssi.ru)

² CRAL, UMR 5574 du CNRS, Ecole Normale Supérieure de Lyon, 46 allée d'Italie, 69364 Lyon Cedex 07, France (gmassacr@ens-lyon.fr)

³ Observatoire de Haute Provence, CNRS, 04870 Saint Michel l'Observatoire, France (gillet@obs-hp.fr)

Received 12 July 1999 / Accepted 16 November 1999

Abstract. The radiative cooling of a shock wake under typical conditions of stellar atmospheres is considered. A simplified model of the radiative relaxation zone is used, and the transfer equation is solved for the line radiation across the shock. Using this solution, the contribution of spectral lines to the radiative cooling is studied, including the elements H, He, C, N, O, Na, Mg, Si, S, Ca and Fe. The line cooling rate is found to be always high in a zone of optical depth unity behind the front. We show that in this zone the relative contribution from each line to the total energy loss mainly depends on the local conditions (density, temperature, postshock gas velocity) and on the line wavelength, but is independent of the line strength. Consequently, the cooling by elements having many line transitions can be very effective. A preliminary analysis shows that the cooling due to Fe lines considerably reduces the spatial extent of the radiative shock wake with respect to the one obtained with H⁻ and H continua. A more sophisticated analysis is needed to determine the exact thermal structure of the wake, which will be the subject of a forthcoming paper.

Key words: radiative transfer – shock waves

1. Introduction

One of the most important problems in stellar radiative gas-dynamics is to estimate the energy exchange rate between matter and radiation field. This rate is especially needed for shock structure analyses, when departures from local thermodynamic equilibrium (LTE) and radiative equilibrium become large. Radiative cooling of the gas in the shock wake and heating in the precursor are the major factors determining the thermal structure of the shock. The knowledge of this structure is necessary for the interpretation of the shock-induced spectroscopic phenomena observed in yellow and red giants, especially the emission in the Balmer and some other lines. Unfortunately, the full self-consistent problem of the radiative shock structure is not resolved yet due to immense technical difficulties. Up to now only more or less approximate solutions have been obtained.

Whitney & Skalafuris (1963) and Skalafuris (1965, 1968) have studied a limited problem of the effect of continuum ra-

diation on the precursor and wake in a non-LTE hydrogen gas. Hill (1972) considered the same problem under the LTE assumption. A more sophisticated analysis has been attempted by Narita (1973), who estimated the radiative losses due to the Lyman and Balmer continua behind the shock front. Klein et al. (1976, 1978) obtained a self-consistent solution of this problem for the radiative wake of a hydrodynamic shock under more realistic stellar conditions. Unfortunately, their coarse zoning did not allow them to consider the radiative precursor and the detailed structure of the thermalization zone. For this reason, their approach was limited to the atmospheres of A-type and hotter stars, where the ionization degree of the unperturbed gas is relatively high. However, as shown by Gillet et al. (1989 and references therein), the whole shock structure is very sensitive to the degree of ionization in the precursor, especially if it was initially weak. Consequently, all physical processes in this zone should be treated very accurately, and simultaneously with the postshock region. Recently, Fadeyev & Gillet (1998) proposed a general iterative method to obtain a self-consistent solution of the equations of fluid dynamics, radiative transfer and atomic kinetics for a steady-state radiative shock in partially ionized hydrogen gas. They take into account the frequency-dependence of the radiation continua contrary to Narita (1973) or Huguet & Lafon (1997), where the Lyman and Balmer continua were replaced by a “mean” photon (Gillet 1999). A generalization to a multi-level atom, which will permit the calculation of line profiles, is now available (Fadeyev & Gillet 2000).

The main difficulty of the problem of the radiative cooling in low-temperature stellar atmospheres is that one should consider all possible atomic transitions of all species which can absorb radiation. In the past studies devoted to radiative shocks, mostly pure gases were considered, such as hydrogen, neon or argon. For a hydrogen gas under typical conditions of stellar atmospheres, i.e. $10^{-12} \text{ g cm}^{-3} < \rho < 10^{-7} \text{ g cm}^{-3}$, $5000 \text{ K} < T < 10000 \text{ K}$, radiative losses in subordinate continua are more important. Indeed, due to very high opacities of the Lyman transitions, there is almost perfect radiative equilibrium in the Lyman lines and Lyman continuum. In an optically thick case, which is typical for stellar shocks, the cooling due to Balmer and higher subordinate lines is also inefficient compared to that in the optically thin H and H⁻ continua because their pho-

tons are mostly blocked in the wake. However, the metals and other heavy elements in principle can provide an additional and effective source of radiative cooling, due to their innumerable bound-bound transitions in which the stellar gas is not very optically thick. The problem is complicated by the fact that the strongest and the weakest lines do not contribute effectively to the cooling or heating, while the effect of the intermediate lines can be estimated only after a detailed transfer calculation. Because of this difficulty, up to now the optically thin case has been essentially considered in the literature, which is not applicable to stellar atmospheres, but only to high chromospheres or coronae.

Cox & Tucker (1969) have considered the radiative cooling rate in a low-density, high-temperature plasma with cosmic abundances. They included free-free, bound-free and bound-bound transitions for several elements. However, the specific physical conditions adopted in their calculations ($T > 10^4$ K) are not valid for atmospheres of cool and normal stars. Also, the authors assumed the gas to be optically thin to all frequencies and ignored certain important elements, such as Fe, Ti, Ba etc. Later, McWhirter et al. (1975) performed calculations of the radiative losses in the solar chromosphere and corona (always for the optically thin case), including iron bound-bound transitions, and obtained similar results. A general review of the radiative cooling problem in stellar plasmas can also be found in Praderie (1981). In the optically thin case, the major contributors to the radiative cooling are Ly α , Ca II and Mg II resonant lines, while under typical conditions of normal and cool atmospheres, the photons in these lines are blocked due to high opacity, and do not contribute to the cooling.

Recently Voitke et al. (1996) have studied, under the Sobolev approximation, the radiative cooling in low-temperature stellar winds. Their method allows to relax the LTE approximation and to include in principle such calculations in a hydrodynamic modelling. One of their conclusions is that at $\rho \geq 10^{-12}$ g cm $^{-3}$ and $T \geq 5000$ K the radiative cooling occurs mainly in the H and H $^-$ b-f continua. Unfortunately, only a few dozen lines have been included in their analysis (e.g. only 15 IR lines of Fe I and Fe II), and the optical depths effect were ignored for the continua, resulting in an overestimation of the continuum cooling in dense atmospheres. Also, specific conditions in the shock waves (steep Doppler shift etc.) do not allow to apply the above results to stellar shocks.

In this first paper we attempt a simplified analysis of the radiative cooling in lines and continua in a radiative shock wake for typical conditions of stellar atmospheres. We neglect the atomic kinetics and restrict the problem to the zone of radiative relaxation. We consider the problem of the line radiation transfer through a steady-state shock in a plane-parallel geometry. In Sect. 2 we review some general aspects of the shock structure and major physical processes in the postshock region. In Sect. 3 we describe our simplified shock wave model and study the cooling effect of one spectral line following the solution of the transfer equation. The radiative cooling involving many lines is discussed in Sect. 4 and, finally, some conclusions are given in Sect. 5.

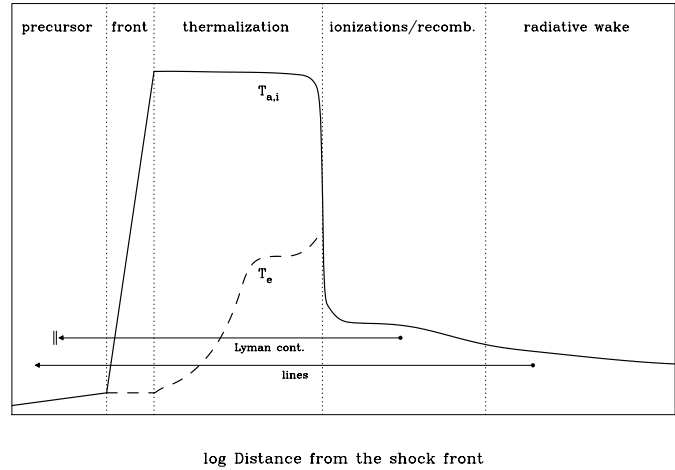


Fig. 1. Schematic diagram showing the different zones of a shock wave and variations of the temperatures of the electrons and heavy particles with approximate logarithmic distance from the shock front

2. General problem

2.1. Fine shock structure and radiative relaxation zone

The shock wave structure can be subdivided into several principal zones with different characteristics, as schematically shown in Fig. 1 (see e.g. Zel'dovich & Raizer 1966). All these zones, except for the much wider zone of radiative relaxation (or *radiative wake*), are normally optically thin in the non-Lyman transitions. Here we briefly describe some important physical processes occurring in each of these zones, following Narita's (1973) work.

Just ahead of the shock front, hydrogen is partly ionized due to absorption of the Lyman continuum radiation emerging from the postshock region. The width of this radiative precursor should be of order of a mean free path of the Lyman photon. Within the viscous jump, or shock front (3-4 mean free paths of heavy particles), both the atomic and ion temperatures ($T_a \approx T_i$) strongly increase, sometimes up to 10^5 K or more depending on the shock velocity, through the action of viscous forces on heavy particles. Because the viscous forces in the electron gas are negligibly small over the shock front, the electrons are not heated by this process. In fact, because electrons and ions are strongly bound together by electric forces, the electron gas is adiabatically heated at a small rate, up to 2.5 for the strongest shocks. Nevertheless, if the electron conductivity is not negligible, the heating of the electrons in the preshock region can be even more efficient than this adiabatic heating (Zel'dovich & Raizer 1966, § VII.2.12).

In the thermalization zone, T_e begins to rise due to elastic collisions with atoms and ions. Once the electron temperature is sufficiently large, collisional excitations and ionizations by electrons start which brings down T_e . As a result of elastic collisions of electrons with atoms and ions, T_a and T_i strongly decrease.

After thermalization ($T_e = T_a = T_i$), when ionization has reached its maximum, a quasi-equilibrium state appears (Narita

1973, Fadeyev & Gillet 1998). When subsequent recombinations and following de-excitations occur, they are not exactly compensated by the reciprocal processes which lead to radiative losses in the Lyman, Balmer and other subordinate continua and spectral lines. When the ionization coefficient $N(H^+)/N(H^0)$ drops to a few percent (at a distance of about 10^5 - 10^6 cm from the front), the decrease of the gas temperature, which is near 10000 K, slows down.

The next zone of the wake is still far from radiative equilibrium. It is partially transparent in the Balmer and higher continua and in weak spectral lines, which cools the gas. This part of the wake can be called the *cooling radiative wake*. It is the most important zone with respect to the formation of the observed emission lines in pulsating stars. Indeed, all previous zones are optically thin to the non-Lyman radiation, so their relative contribution ΔI_ν to the total emergent intensity is negligible. On the contrary, the cooling radiative wake in stellar atmospheres is usually very optically thick in the Balmer and some other strong lines ($\Delta\tau \approx 10^2$ or more). Consequently, the observed shock-induced emission in these lines should reflect, at least in part, the thermal conditions in this zone. Here, an understanding of the radiative cooling in this zone is very important for the determination of the true shock structure and interpretation of the spectral peculiarities of the pulsating stars.

2.2. Gas energy balance and transfer equation

As shown by Castor (1972), the energy equation for gas and radiation in a spherically-symmetric co-moving frame, without thermal conductivity, viscosity and convection, and to order $O(v/c)$ is

$$\frac{D(e_g + e_r)}{Dt} + (p_g + p_r) \frac{D(1/\rho)}{Dt} - \left(\frac{3p_r}{\rho} - e_r \right) \frac{v}{r} = -\frac{1}{\rho} \nabla \cdot \mathbf{F}_{\text{rad}}, \quad (1)$$

where e_g and $e_r = 4\pi J/\rho c$ are the gas and radiation energy per gram, respectively, p_g and $p_r = 4\pi K/c$ the gas and radiation pressure, J and K the zero and the second frequency-integrated moments of the specific intensity I_ν as seen in the co-moving frame, ρ the mass density, $D/Dt \equiv \partial/\partial t + v\partial/\partial r$ is the Lagrangean time-derivative, r and v the Eulerian radius and local fluid velocity, and \mathbf{F}_{rad} the frequency-integrated radiative flux. Note, that e_g includes both translational and inner degrees of freedom of atoms.

From the zero moment of the non-stationary co-frame transfer equation (Castor 1972), one gets the energy equation for the radiation alone

$$\frac{De_r}{Dt} + p_r \frac{D(1/\rho)}{Dt} - \left(\frac{3p_r}{\rho} - e_r \right) \frac{v}{r} = -\frac{1}{\rho} \nabla \cdot \mathbf{F}_{\text{rad}} - \frac{4\pi}{\rho} \int_0^\infty (\chi_\nu J_\nu - \eta_\nu) d\nu, \quad (2)$$

where χ_ν and η_ν are the true absorption and emission coefficients, which are supposed isotropic in the co-moving frame,

and J_ν is the frequency-dependent mean intensity. From Eqs. (1) and (2) one can see that the energy equation for the gas is

$$\frac{De_g}{Dt} + p_g \frac{D(1/\rho)}{Dt} = \frac{4\pi}{\rho} \int_0^\infty (\chi_\nu J_\nu - \eta_\nu) d\nu. \quad (3)$$

For a plane-parallel flow ($r \rightarrow \infty$), to which we restrict our analysis of a stationary shock wave, Eqs. (1) and (2) reduce to the same Eq. (3). This equation gives the rate of temperature variation in the gas due to radiative and adiabatic losses. The second term in the left of Eq. (3) describes the adiabatic work produced by the gas per second, while the integral stands for the heat exchange rate between the matter and the radiation field. The adiabatic term depends on specific conditions of the gas motions and in principle can be easily estimated once the thermodynamic and hydrodynamic parameters are known. Although this cooling mechanism can be very effective in low-density atmospheric regions, in this paper we shall confine our attention to the radiative losses only.

The cooling rate of the gas due to radiative processes only is thus

$$\left(\frac{De_g}{Dt} \right)_{\text{rad}} \equiv \frac{4\pi}{\rho} \int_0^\infty (\chi_\nu J_\nu - \eta_\nu) d\nu. \quad (4)$$

Adopting the full redistribution in the line, the coefficients of absorption χ_ν and emissivity η_ν can be written as

$$\chi_\nu = \chi_{\nu c} + \sum_l \chi_l \phi_{\nu l} \quad (5)$$

$$\eta_\nu = \chi_{\nu c} B_\nu + \sum_l \chi_l S_l \phi_{\nu l}, \quad (6)$$

where the summation is performed over all lines, $\phi_{\nu l}$ is the isotropic normalized line absorption profile

$$\int_0^\infty \phi_{\nu l} d\nu \equiv 1, \quad (7)$$

and S_l and χ_l are the source function and the absorption coefficient for the l -th line, formed in the $L \rightarrow U$ transition, whose standard expressions are:

$$\chi_l = \left(n_L \frac{\pi e^2}{mc} f_l \right) \left(1 - \frac{g_L n_U}{g_U n_L} \right), \quad (8)$$

$$S_l = \frac{2h\nu_l^3}{c^2} \left(\frac{g_U n_L}{g_L n_U} - 1 \right)^{-1}. \quad (9)$$

$\chi_{\nu c}$ is the continuum absorption coefficient. In Eq. (6), for the sake of simplicity, the continuum source function is substituted by the Planck function $B_\nu(T)$. With Eqs. (5) and (6), the integral in Eq. (4) takes the form

$$\int_0^\infty (\chi_\nu J_\nu - \eta_\nu) d\nu = \int_0^\infty \chi_{\nu c} (J_\nu - B_\nu) d\nu + \sum_l \chi_l (\bar{J}_l - S_l), \quad (10)$$

where

$$\bar{J}_l \equiv \int_0^\infty \phi_{\nu l} J_\nu d\nu \quad (11)$$

is the so-called scattering integral for the l -th line, calculated in the co-moving frame. The integral on the right-hand side of Eq. (10) displays the cooling rate due to continuum, whereas the sum gives the rate due to spectral lines. The mean intensity J_ν is to be evaluated from the co-moving radiative transfer equation in the shock wake, resolved simultaneously with the statistical equilibrium of the atomic populations. However, even for plane-parallel and stationary shocks, the co-moving transfer equation still remains very complicated if the fluid velocity (or density) is not constant in the pre- or postshock regions (Castor 1972).

Actually, the postshock gas velocity v_g , measured in the shock front frame, is not constant and normally decreases with distance from the front as T decreases due to radiative cooling (consequently, the density increases). Indeed, for a plane, stationary shock we can apply the two first Rankine-Hugoniot relations (neglecting the radiation pressure)

$$\rho v_g = C_1, \quad (12)$$

$$P_g + C_1 v_g = C_2, \quad (13)$$

where $P_g = R\rho T/\mu$ is the gas pressure, R is the universal gas constant, μ the molecular weight, and C_1 and C_2 the flow constants. These equations reduce to

$$\frac{T}{\mu} = \frac{v_g}{R} \left(\frac{C_2}{C_1} - v_g \right), \quad (14)$$

which yields that T has a maximum at $v_g = v_* = C_2/2C_1$. Hence, v_g must decrease with the distance from the front due to cooling, only if its value just behind the front does not exceed v_* . Let us denote the postshock Mach number as $M \equiv v_g/c_s$, where $c_s = \sqrt{P_g/\rho}$. Then the condition $v_g < v_*$ transforms into

$$M < \frac{v_*}{c_s} = \frac{1}{2} \left(M + \frac{1}{M} \right), \quad (15)$$

or $M^2 < 1$, which is always valid in the postshock region. Thus, the gas velocity decreases with T as

$$v_g(T) = v_* - \sqrt{v_*^2 - TR/\mu}. \quad (16)$$

For the sake of simplicity, however, in this paper we adopt $v_g = \text{const}$ in the preshock and postshock zones, with a jump at the shock front.

We also neglect all the terms of order $O(v^2/c^2)$ and higher. Thus, in our transfer equation we take into account only the linear Doppler effect produced by the shock. After these simplifications, the transfer equation takes the form

$$\frac{1}{c} \frac{DI_\nu}{Dt} + \mu \frac{\partial I_\nu}{\partial z} = \eta_\nu - \chi_\nu I_\nu, \quad (17)$$

where $I_\nu(\mu, z, t)$ is the specific intensity, $\mu \equiv \cos \theta$ the angular coordinate, and z the linear coordinate. Note that in general η_ν

and χ_ν are functions of both t and z . Although formally, in Eq. (17) the scattering coefficient should be added to χ_ν , here we suppose it is negligible.

Following the reasoning of Mihalas (1978), we also assume that for the line transfer analysis the time derivative, which describes the effect of the delay of radiation, is negligible with respect to the Doppler effect due to the velocity jump at the front. This means that physical quantities in the shock are supposed to vary only slowly in the time required for a photon to cross the cooling radiative wake. Finally, we get the steady-state equation

$$\mu \frac{\partial I_\nu}{\partial z} = \eta_\nu(z) - \chi_\nu(z) I_\nu \quad (18)$$

which shall be used to calculate J_ν and, thus, to evaluate the cooling rate according to Eqs. (4) and (10).

2.3. Continuum radiative cooling

We suppose here that hydrogen, as the most abundant element, is the major contributor to the continuum cooling in stellar shock wakes (except for helium or C-O stars); so we do not consider the continua of other elements.

A detailed discussion of the effect of the H and H⁻ bound-free and free-free continua on cooling was recently given by Voitke et al. (1996). Unfortunately, due to a limitation of the method used (Sobolev approximation), not all the results of this study apply to stellar shocks in the atmospheres of normal and cool pulsating stars. Namely, the Lyman continuum does not efficiently contribute to the cooling of typical shock wakes. Indeed, the absorption coefficient for the photoionization of hydrogen from the level i at the threshold frequency may be written as

$$\chi_{\nu c}^i \simeq 3.3 \cdot 10^6 i^3 e^{-E_i/kT} X_H \rho \text{ [cm}^{-1}\text{]}, \quad (19)$$

where $E_i = 13.6(1 - 1/i^2)$ eV, $X_H = n(H^0)/(n(H^0) + n(H^+))$ is the fraction of neutral hydrogen, and ρ is in g cm⁻³. Here we assumed solar hydrogen abundance, neglected stimulated emission, and set Gaunt factors equal to one. For the conditions of normal stellar atmospheres ($T_{\text{eff}} \approx 5000 - 7000$ K), X_H is close to one. Hence, for a typical geometrical extension of the dense atmospheric region of 10^{10} cm, assuming a mean density $\rho \simeq 10^{-11}$ g cm⁻³, the optical depth of the shock front in the Lyman continuum is $\tau_c^{\text{Ly}} \simeq 10^5$. In the radiative wake, assuming $T = 8000$ K and $\rho = 10^{-8}$ g cm⁻³, we get $\chi_{\nu c}^{\text{Ly}} \simeq 3.3 \cdot 10^{-2}$ cm⁻¹. Thus, already at the distance of 10^4 cm from the front, these photons are blocked and cannot contribute to the cooling of the shock (Narita 1973), so that we can neglect the frequency range corresponding to the Lyman continuum in Eq. (4). For the same reason, the contribution of the Lyman lines to the cooling rate vanishes ($\tau_{\text{Ly}\alpha} \simeq 10^{10}$). Note that although S_ν for these lines can considerably deviate from B_ν even at large optical depths, the frequency-integrated value of S very quickly tends to \bar{J} (already at $\tau_{\text{Ly}\alpha} \simeq 10^5$) due to strong scattering in these lines.

In stellar atmospheres, the Balmer and higher continua are much more transparent, because of the low population of the rel-

evant levels. For example, according to Eq. (19), at $T = 5000$ K (typical preshock temperature) one has: $\chi_{\nu c}^{\text{Ba}}/\chi_{\nu c}^{\text{Ly}} = 4.2 \cdot 10^{-10}$ and $\chi_{\nu c}^{\text{Pa}}/\chi_{\nu c}^{\text{Ly}} = 1.7 \cdot 10^{-12}$, which results in an optical depth of the front much smaller than one. The optical thickness of the wake is normally of the same order or less. The opacity due to H^- absorption for $T \approx 5000$ K and $\rho \approx 10^{-10} \text{ g cm}^{-3}$ is about an order of magnitude larger than that in the Balmer continuum, but the wake still remains optically thin. Thus, these continua can well contribute to the cooling.

On the other hand, because of the relatively low opacity, the deposition of the thermal emission on the emerging radiation in the optically thin domains would be small. Hence, one can expect that, in the shock wake, J_ν remains almost unaffected, i.e. $J_\nu \ll B_\nu$ under LTE. Consequently, in the integral of the right-hand side of Eq. (10), we can neglect J_ν with respect to B_ν . Also, because the Planck mean opacity

$$k_{PC} \equiv \int_0^\infty \chi_{\nu c} B_\nu d\nu / \int_0^\infty B_\nu d\nu, \quad (20)$$

calculated including continua only and without Lyman continuum contribution, is normally close to the Rosseland mean

$$\chi_R \equiv \left(\int_0^\infty \frac{1}{\chi_\nu} \frac{dB_\nu}{dT} d\nu / \int_0^\infty \frac{dB_\nu}{dT} d\nu \right)^{-1}, \quad (21)$$

we get a useful approximation of this integral in the wake under LTE

$$\left(\frac{De_g}{Dt} \right)_{\text{cont}} = \frac{4\pi}{\rho} \int_0^\infty \chi_{\nu c} (J_\nu - B_\nu) d\nu \approx -\frac{4\pi}{\rho} \chi_R B(T), \quad (22)$$

where $B(T) = \sigma_R T^4 / \pi$, σ_R is the Stefan-Boltzmann constant. We see, that in approximative calculations of the continuum cooling in stellar atmospheres it is more appropriate to use the *Rosseland* mean opacity. Indeed, the use of the full Planck mean opacity would not take into account the blocking of photons in the opaque domains of the spectrum and would overestimate the cooling rate by several orders of magnitude. The Rosseland mean, because of its specific averaging, accounts for the opacity minima (i.e. the transparent continua), and is more relevant. The cooling time for the continuum can then be estimated as

$$t_{\text{cont}} = \frac{e_g}{\langle De_g/Dt \rangle_{\text{cont}}} \approx \frac{e_g \rho}{4\pi \chi_R B(T)}. \quad (23)$$

For instance, for $T = 5000$ K and $\rho = 10^{-10} \text{ g cm}^{-3}$ $\chi_R \approx 10^{-13} \text{ cm}^{-1}$, and t_{cont} is about $4 \cdot 10^3$ s. However, without LTE, the cooling rate may differ from (23), because the atomic populations and, more importantly, the electronic concentration n_e would be different. For instance, Voitke et al. (1996) found that the cooling rate is overestimated in LTE by 1-2 orders of magnitude for the above values of T and ρ . A further non-LTE transfer analysis is needed to clarify this important question.

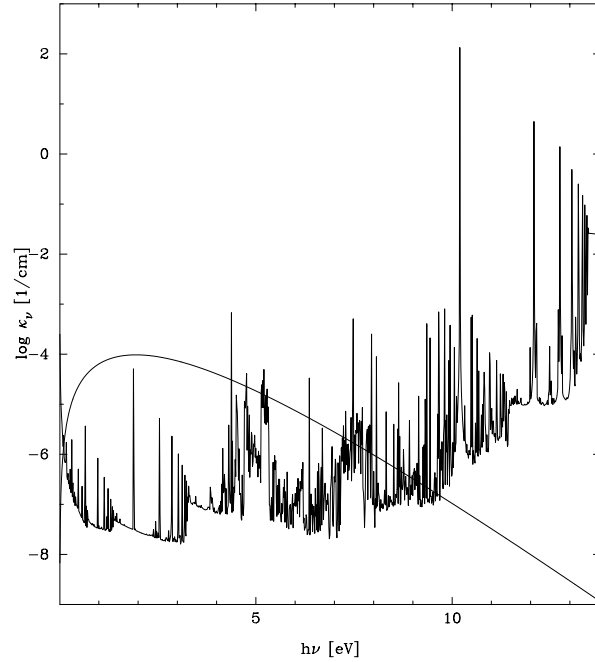


Fig. 2. Absorption spectrum for solar abundance, $T = 8000$ K and $\rho = 10^{-8} \text{ g cm}^{-3}$. We also show the logarithm of the Planck function $B_\nu(T)$ (in $\text{erg cm}^{-2} \text{ s}^{-1} \text{ Hz}^{-1} \text{ sr}^{-1}$)

3. Transfer analysis for one line

The cooling rate due to spectral lines, according to (10), can be expressed as

$$\left(\frac{De_g}{Dt} \right)_{\text{lines}} = \frac{4\pi}{\rho} \sum_l \chi_l S_l (\bar{J}_l / S_l - 1). \quad (24)$$

The problem is thus to calculate \bar{J}_l / S_l in the shock wake for each spectral line, and to perform the sum (24) over all lines.

As an example, a typical monochromatic absorption spectrum for solar abundances, $T = 8000$ K and $\rho = 10^{-8} \text{ g cm}^{-3}$ is presented in Fig. 2. It is computed including elements H, He, C, N, O, Na, Mg, Si, S, Ca and Fe; data for bound-bound transitions (around 2 million lines) and photoionizations have been taken from TOPbase (Cunto et al. 1993), the atomic data base computed by the Opacity Project group (Seaton 1987), except for Fe I and Fe II lines which come from the Kurucz compilation. In this figure, apart from strong Lyman lines, one can see two broad UV Fe line packets at $h\nu/kT \approx 7$ and $h\nu/kT \approx 11$ ($\lambda \approx 2600 \text{ \AA}$ and 1600 \AA , respectively). These packets are located at frequencies where the Planck function is not negligible while the opacities of most of these lines are not as strong as those of the Lyman lines. Thus, even if the Lyman photons are blocked, one can expect an increase of the cooling rate due to these numerous weak lines, provided that the radiation in these lines is not blocked.

The major difficulty of such a calculation is that the shock structure should be determined simultaneously with the cooling rate, which is very sensitive to the optical depths in different lines. As a first step, here we perform a restricted analysis of a single line transfer problem for a simplified shock model and

obtain \overline{J}_l/S_l (which will be simply written as \overline{J}/S hereafter) as a function of the different parameters of the model. Next, in Sect. 4, we apply these results to a preliminary analysis of the radiative cooling due to the whole line spectrum.

3.1. Simplified model for a radiative shock wake

We search for the solution of the line transfer equation (18) through a steady-state shock, which has a structure which is supposed to be known. We neglect all optically thin (for non-Lyman radiation) shock zones, reducing thus the wake model to the radiative cooling region only (see Fig. 1). So our “front”, treated here as a discontinuity, includes the radiative precursor, the viscous front and the thermalization zone in which excitations and ionizations mainly occur. Finally, our model consists of three regions: the unperturbed preshock atmosphere, the radiative wake, and the postshock region where the temperature is already relaxed to the ambient level (see Fig. 3).

Other major simplifications are:

- plane-parallel geometry;
- constant (though different) velocities in the preshock and postshock zones. The velocity jump Δv_s at the “front” is one of the parameters of the problem. In the present analysis Δv_s was varied from 0 to 80 km/s;
- complete redistribution in the line with the Gaussian absorption profile

$$\phi(\nu) = \frac{1}{\sqrt{\pi}\Delta\nu_D} e^{-(\nu-\nu_l)^2/\Delta\nu_D^2}, \quad (25)$$

which is relevant for weak lines. The Doppler width $\Delta\nu_D$ is supposed constant and is estimated with $T = 4500$ K and $\lambda = 5000$ Å. In fact, only the ratio of Δv_s to the Doppler velocity $c\Delta\nu_D/\nu_l$ is important. With the previous values this ratio varies from 0 to about 10. We should note, however, that the effect of this ratio is negligible in the wake, if it only exceeds ≈ 2 ;

- we assume that the ratio of the opacity in the center of the line to that in the nearby continuum, $\chi_l\phi(\nu_l)/\chi_{\nu c}$, is constant within the whole atmosphere. This ratio mainly depends on the relative populations of the respective absorbers and these populations are roughly proportional to the density in the variation range of the shock conditions. The total line absorption is the superposition of the Doppler and continuum absorptions, so the above ratio characterises the relative strength of the line. We varied this parameter in the range from a few units to 10^5 , but no perceptible influence on the cooling rate was found, apart from the trivial changing of the optical depth scale;
- we assume the source function, $S_\nu \equiv \eta_\nu/\chi_\nu$, to be independent of ν within the line profile. It means that the source functions in the line and the nearby continuum are the same. In principle, this is correct only in the LTE case, but we assume it to be approximately correct at least for a large number of low-excitation lines, because in this case the bound-bound photon diffusion (the main process breaking the LTE) must not be very efficient;

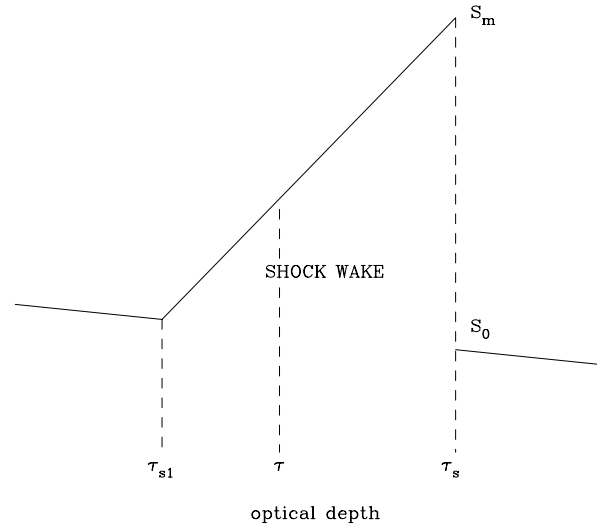


Fig. 3. Schematic representation of the source function S for the shock model used in this paper. The optical depth scale is linear

- in the ambient atmosphere *beyond* the wake we adopt a linear law for $S(\tau)$,

$$S(\tau) = A_0\tau + B_0, \quad (26)$$

where τ , the static optical depth in the center of line, is defined by

$$d\tau \equiv -(\chi_l\phi(\nu_l) + \chi_{\nu c}) dz. \quad (27)$$

The form of $S(\tau)$ in the wake cannot be known *a priori* because it must depend on the unknown cooling rate. For the sake of simplicity, we also adopt a linear form for it, but with different parameters A_0 and B_0 (see Fig. 3), so that at the front the source function is characterised by a jump $\Delta S = S_m - S_0$. In the present analysis $\log(S_m/S_0)$ was varied from 0 to 2, the last value corresponding to a jump of B_ν as temperature rises from 4500 to 15,000 K at $\lambda = 5000$ Å.

The last two parameters of the problem are the static optical depth of the “front”, τ_s , and the one of the inner boundary of the wake, τ_{s1} , both measured in the line center. In the following we shall also use the optical width of the wake, $\Delta\tau_s \equiv \tau_{s1} - \tau_s$. Note that for a given shock, this width is different from one line to the other. However, under our hypotheses, the ratio τ_{s1}/τ_s is equal to that of the nearby continuum and thus approximately constant for lines in the same frequency domain.

The relation between $S(\tau)$ and $T(\tau)$ in the shock wake will not be discussed in this paper. We only note here, that although in the case of pure diffusion (typical for very strong lines) the line source function has nothing in common with the local temperature, for weak lines with not too high excitation energies, especially in dense atmospheric regions, they must be closely related. We assume that S should have a maximum immediately behind the “front”, and then decrease as optical depth increases.

3.2. Method of solution

To find the specific monochromatic intensities in both the preshock and postshock regions, we use the formal solution of the transfer equation (18) (e.g. Mihalas 1978)

$$I(\tau_\nu, \nu, \mu) = I(\tau_{\nu 0}, \nu, \mu) e^{(\tau_\nu - \tau_{\nu 0})/\mu} + \int_{\tau_\nu}^{\tau_{\nu 0}} S(t, \mu, \nu) e^{(\tau_\nu - t)/\mu} \frac{dt}{\mu}. \quad (28)$$

Here τ_ν is the optical depth at frequency ν , which depends on the direction μ because of the Doppler shift, and which is defined by

$$d\tau_\nu \equiv -(\chi_l \phi(\nu[1 - \mu v/c]) + \chi_{\nu c}) dz, \quad (29)$$

where v is the local velocity. In order to account for the variations of the optical depth scale due to both the line profile and the Doppler jump at the front, we introduce a function

$$f \equiv \frac{\chi_l \phi(\nu[1 - \mu v/c]) + \chi_{\nu c}}{\chi_l \phi(\nu_l) + \chi_{\nu c}}, \quad (30)$$

so that the optical depth τ_ν is related to the static optical depth τ in the line center as

$$d\tau_\nu = f d\tau. \quad (31)$$

Because the line-to-continuum opacity ratio is assumed constant, and the velocity structure of the shock model is very simple ($v = \Delta v_s$ in the postshock and $v = 0$ in the preshock region), f depends on the position in a trivial way. The formal solution of the radiative transfer then reads

$$I^-(\tau, \nu, \mu) = I^-(\tau_1, \nu, \mu) e^{(\tau - \tau_1)f/\mu} - \int_{\tau_1}^{\tau} S(t) e^{(\tau - t)f/\mu} \frac{f dt}{\mu}, \quad (32)$$

$$I^+(\tau, \nu, \mu) = I^+(\tau_2, \nu, \mu) e^{(\tau - \tau_2)f/\mu} + \int_{\tau}^{\tau_2} S(t) e^{(\tau - t)f/\mu} \frac{f dt}{\mu}, \quad (33)$$

where I^+ and I^- are the intensities in the positive ($\mu > 0$) and negative ($\mu < 0$) directions. Eqs. (32) and (33) hold when both points τ and τ_1 , or τ and τ_2 , lie in the same region of constant v . Integration for I^- is started with $I^- = 0$ at the outer boundary of the atmosphere ($\tau_1 = 10^{-4}$), and pursued by stages down to the inner boundary ($\tau_2 \approx 10^5$) where we assume $I^+ = I^- = S(\tau_2)$. Then I^+ is integrated from the inner to the outer boundary. The function f undergoes a jump at the shock front, according to Eq. (30).

The calculations are performed with 16 angular, 101 frequency and 500 spatial nodes. After evaluation of the matrices $I^+(\tau, \nu, \mu)$ and $I^-(\tau, \nu, \mu)$, we calculate the zero moment

$$J_\nu \equiv \frac{1}{2} \left(\int_0^1 I^+ d\mu + \int_{-1}^0 I^- d\mu \right) \quad (34)$$

by Gauss quadratures, and then the scattering integral \bar{J} using Eq. (11).

3.3. Results

3.3.1. Analytical approach

The general behavior of \bar{J}/S can be studied analytically by putting a simplifying assumption $A_0 = 0$ in Eq. (26), which means a constant source function off the wake. With this, the mean intensity in the wake (and behind) writes

$$J(\tau, \nu) = S(\tau) - \frac{S_0}{2} \int_0^1 d\mu e^{-\tau_s f_1/\mu} e^{(\tau_s - \tau) f_0/\mu} - \frac{\Delta S}{2} \left\{ E_2([\tau - \tau_s] f_0) + \frac{E_3([\tau - \tau_s] f_0) - E_3(|\tau_{s1} - \tau| f_0)}{f_0 \Delta \tau_s} \right\}, \quad (35)$$

where f_1 and f_0 are functions defined in (30) and calculated with $v = \Delta v_s$ and $v=0$ respectively, $\Delta S = S_m - S_0$ is the source jump and

$$E_n(x) = \int_1^\infty \frac{\exp(-xt)}{t^n} dt \quad (36)$$

is the n -th exponential integral. Physically, the integral in the first line originates from the propagation of the downward radiation I^- from the preshock region into the wake. This is the only term involving the Doppler jump at the front (through f_1). The second line also comes from I^- and is due to the propagated effect of the source jump ΔS . The last line originates from radiation propagating in both directions and is related to the slope $\Delta S/\Delta \tau_s$ of the source function in the wake.

After integrating Eq. (35) over ν with the normalized line absorption profile ϕ_ν as the weight function, we get

$$\frac{\bar{J}(\tau)}{S(\tau)} = 1 - \frac{S_0}{2S(\tau)} \int_0^\infty d\nu \phi_\nu \int_0^1 d\mu e^{-\tau_s f_1/\mu} e^{(\tau_s - \tau) f_0/\mu} - \frac{\Delta S}{2S(\tau)} \int_0^\infty d\nu \phi_\nu \left\{ E_2([\tau - \tau_s] f_0) + \frac{E_3([\tau - \tau_s] f_0) - E_3(|\tau_{s1} - \tau| f_0)}{f_0 \Delta \tau_s} \right\}. \quad (37)$$

Several important conclusions follow from (37) for the behaviour of \bar{J}/S :

- without the shock ($\Delta S = 0$, $f_1 = f_0$), we obtain

$$\frac{\bar{J}(\tau)}{S(\tau)} = 1 - \frac{1}{2} \int_0^\infty \phi_\nu E_2(\tau f_0) d\nu, \quad (38)$$

which describes the solution in a static atmosphere; \bar{J}/S lies between 1/2 ($\tau \ll 1$) and 1 ($\tau \gg 1$).

- the dependence of \bar{J} on the source function jump ΔS is linear. The related term does not depend on the velocity jump at the shock front, nor directly on the optical depth τ_s of the front, but only on the optical depth $\tau - \tau_s$ from the front and on the optical width $\Delta \tau_s$ of the wake;
- the optical depth of the front τ_s intervenes only in the first integral on the right through the combination $\tau_s f_1$. For a very strong velocity jump, f_1 can be considered as independant

of μ because of the profile ϕ_ν . The μ -integral can then be replaced by $E_2(\tau_{sc} + (\tau - \tau_s))$ where τ_{sc} is the optical depth of the front *in the continuum*.

It is also interesting to examine some simple limits obtained from (37) with the assumption of a high velocity jump:

1) $\tau \rightarrow \tau_s$. This case corresponds to the postshock region immediately behind the front. Using the limits $E_2(x) \rightarrow 1$ and $E_3(x) \rightarrow 0.5 - x$ when $x \ll 1$, and $E_2(x), E_3(x) \rightarrow 0$ when $x \rightarrow \infty$, we get

$$\frac{\bar{J}}{S} = \begin{cases} S_0/2S_m & \text{if } \tau_{sc} \ll 1 \text{ and } \Delta\tau_s \ll 1 \\ 0.5 & \text{if } \tau_{sc} \ll 1 \text{ and } \Delta\tau_s \gg 1 \\ 0.5 + S_0/2S_m & \text{if } \tau_{sc} \gg 1 \text{ and } \Delta\tau_s \gg 1 \end{cases} \quad (39)$$

A last case ($\tau_{sc} \gg 1$ and $\Delta\tau_s \ll 1$) would give $\bar{J}/S = S_0/S_m$ but is quite unphysical. For $S_m \gg S_0$ and just behind the front, we may conclude that $\bar{J}/S - 1$ lies between -1 and -0.5 .

2) $\tau - \tau_s \gg 1$. In this case, implying an optically thick wake, we obtain approximately (using a rectangular absorption profile ϕ_ν and the limits $E_2(x), E_3(x) \rightarrow e^{-x}/x$ if $x \rightarrow \infty$)

$$\frac{\bar{J}(\tau)}{S(\tau)} \simeq 1 - \frac{S_0}{2S(\tau)} \frac{e^{-(\tau-\tau_s)} e^{-\tau_{sc}}}{\tau - \tau_s} - \frac{\Delta S}{2S(\tau)} \left(\frac{e^{-(\tau-\tau_s)}}{\tau - \tau_s} - \frac{E_3(|\tau_{s1} - \tau|)}{\Delta\tau_s} \right). \quad (40)$$

In the middle of the optically thick wake ($\tau_{s1} - \tau \gg 1$), and therefore at a fixed *geometrical* distance from the front, the cooling rate, proportional to $\chi_l[\bar{J}(\tau)/S(\tau) - 1]$ (see (24)), will exponentially decrease with the increasing opacity of the line.

As τ becomes close to τ_{s1} (i.e. near the lower boundary of the hot wake), we get

$$\frac{\bar{J}(\tau)}{S(\tau)} \simeq 1 + \frac{\Delta S}{4S_0} \frac{1}{\Delta\tau_s}, \quad (41)$$

and we see that $\bar{J}/S - 1$ becomes *positive*, which means heating of the gas by radiation from the hot part of the wake. This heating is due to the absorption of the hot *line* radiation coming from the wake. Note that the classic heating effect in the preshock region (Mihalas 1969; Narita 1973), on the contrary, is mainly due to the absorption in the line of the *continuum* radiation, coming from the optically thick wake. This preshock heating seems to be more complicate, as we shall see in the next section.

As mentioned above, numerical calculations for the Doppler absorption profile show that the cooling rate in the wake depends very weakly on the line-to-continuum opacity ratio. The above results also suggest that for $S_m \gg S_0$ the dependence of the cooling rate on the velocity jump Δv_s and on τ_s is negligible. Thus, the most important parameters are the optical distance from the front $\tau - \tau_s$, the optical width of the wake $\Delta\tau_s$, and the amplitude of the source function ΔS .

3.3.2. Numerical calculation

Figs. 4, 5 and 6, based on the numerical calculations, represent typical behaviours of \bar{J}/S for different jumps of the source function and for different shock locations. The velocity jump in these

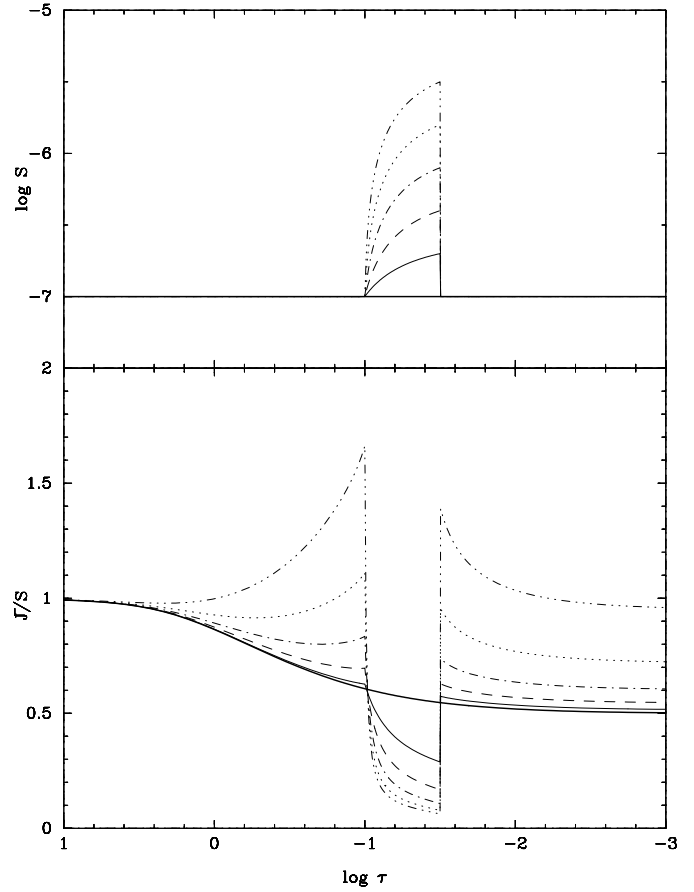


Fig. 4. Variation of \bar{J}/S for different source function jumps ΔS for an optically thin shock with $\Delta v_s = 50$ km/s and $\log \tau_{s1}/\tau_s = 0.5$. The corresponding source functions are shown above. The thick curve shows the solution without shock. $\log S_m/S_0$ increases by steps of 0.3

figures is 50 km/s, and $S_0 = 10^{-7}$ erg cm $^{-2}$ s $^{-1}$ Hz $^{-1}$ sr $^{-1}$. As shown above, the choice of S_0 is not important because \bar{J}/S does not depend on S_0 , but only on S_m/S_0 .

In these figures we also show with a thick line the solution without shock, i.e. with $\Delta S = \Delta v_s = 0$, given by Eq. (38). Without shock, \bar{J}/S reveals a large depression towards the surface, approximately as $\bar{J}/S \approx (1+6\tau)/(2+6\tau)$. In the optically thick region ($\tau \geq 10$) radiative equilibrium holds ($\bar{J} \rightarrow S$), whereas near the surface $\bar{J}/S \rightarrow 0.5$. Because $\bar{J}/S \leq 1$ at all optical depths, this means that in a static regime the lines cool the gas.

In the presence of a shock the cooling in the wake is always stronger than in the static case. In this paper we shall discuss only the “absolute” line cooling effect, i.e. the deviation of \bar{J}/S from unity.

For an optically thin shock (Figs. 4 and 6) the gas cools almost everywhere in the wake, with \bar{J}/S depending mostly on the amplitude of the source function jump ΔS , in agreement with the above analytical solution. In an optically thick shock (Fig. 5), photons are blocked and the cooling in the most part of the wake is negligible. Usually, at a distance of about $\Delta\tau \approx 1-5$ from the shock front, the gas already returns to the radiative

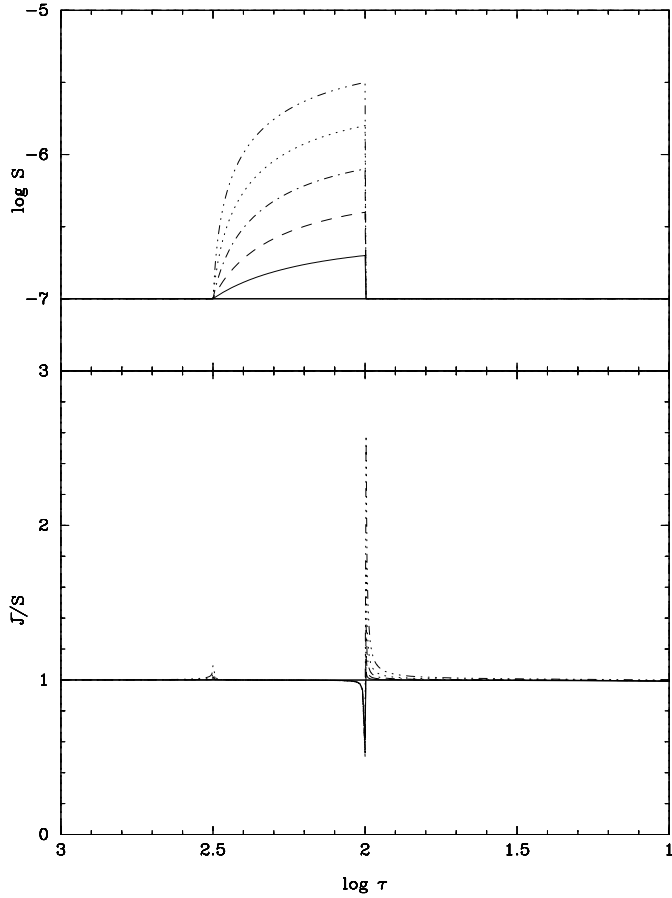


Fig. 5. Same as Fig. 4 but for an optically thick shock

equilibrium in the line, similarly to the static case. However, within the $\Delta\tau \leq 1$ region the lines can cool effectively.

Fig. 7 shows typical variations of \bar{J}/S at the maximum of S just behind the front as a function of the static optical depth of the front, τ_s . These results are obtained for the case $\log \tau_{s1}/\tau_s = 1.0$. In agreement with the analytical result, even at large front depths ($\tau_s \gg 1$), there is a perceptible cooling rate ($\bar{J}/S \approx 0.5$ for large enough S_m). Calculations show that this rate extends up to a distance $\Delta\tau \leq 1$ from the front. Indeed, one of the reasons is that in the optically thick case at small optical distances behind the front the line radiation freely escapes in the upstream direction in the continuum frequencies, because the preshock gas becomes transparent in the line due to the Doppler shift. Thus, $I^+ \gg I^-$ in the wake, which under LTE ($I^+ = B_\nu$) gives

$$\frac{\bar{J}}{S} \approx \frac{I^+ + I^-}{2B_\nu} \approx \frac{1}{2}. \quad (42)$$

Moreover, as follows from Eq. (37) and asymptotic solution 1) for an optically thick shock, even *without velocity jump* cooling would exist within this zone if S_m is large enough. Indeed, the intensity of the radiation, emitted by the hot wake, can be characterized by a color temperature T_w which is higher than

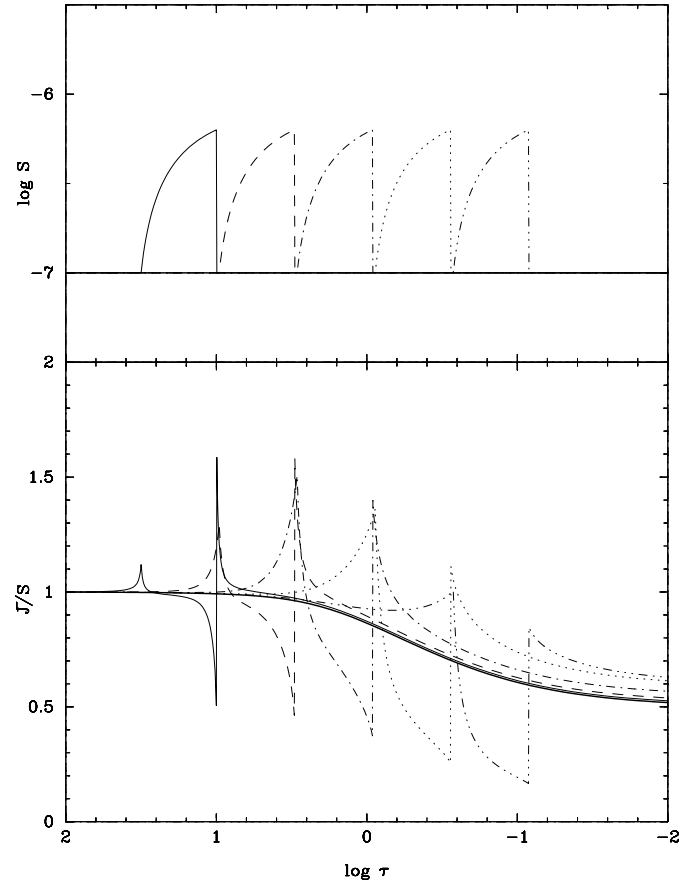


Fig. 6. Same as in Figs. 4 and 5 but for different shock positions. Note that the different curves would correspond, for the same shock, to lines with different opacities

the preshock temperature T . Under LTE we have $I^- \approx B_\nu(T)$ and $I^+ \approx B_\nu(T_w)$, which yields

$$\frac{\bar{J}}{S} \approx \frac{B_\nu(T_w) + B_\nu(T)}{2B_\nu(T_w)} \approx \frac{1}{2} \quad \text{for } B_\nu(T_w) \gg B_\nu(T). \quad (43)$$

3.3.3. Cooling of the moving gas

As an element of gas enters the postshock region, it starts cooling with the locally determined rate, and in the same time it keeps moving away from the front. Because its temperature rapidly decreases, the cooling rate diminishes faster than exponentially with the optical distance from the front, $\tau - \tau_s$ (Eq. (40)). As shown above, the gas can effectively cool in the line only while $\tau - \tau_s$ in the line center is less than, or of the order of 1. This parameter approaches unity in a time $t_{pass} \approx 1/(v_g \chi_{\nu 0})$, where v_g is the postshock gas velocity, and $\chi_{\nu 0} = \chi_l \phi(\nu_l)$ is the monochromatic opacity in the line core. For a Doppler absorption profile, which is valid for most of the non-resonant metal lines, t_{pass} can be expressed as

$$t_{pass} \approx \frac{\sqrt{\pi} 4.3 \cdot 10^{-7} \nu \sqrt{T/A_m}}{v_g \chi_l}, \quad (44)$$

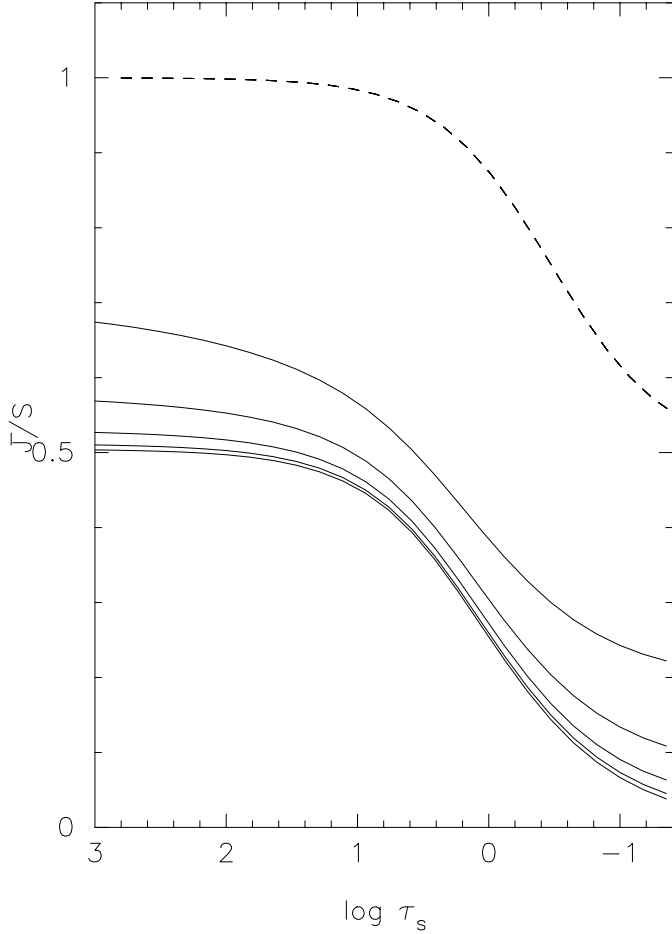


Fig. 7. Solid lines: \bar{J}/S at the S -peak behind the front as a function of the optical depth τ_s of the shock front for $\log \tau_{s1}/\tau_s=1.0$ and for different amplitudes of the source function. $\log(S_m/S_0)$ increases from 0.4 (top) to 2.0 (bottom) with a constant increment of +0.4. Dashed line: the static solution

where A_m is the molecular weight of the species. Thus, only during this time the gas cools by the line radiation. The total amount of the gas energy (per gram) which is lost through one line radiation during the passage of the gas element across the whole postshock region, according to Eq. (24) and under LTE, is

$$\Delta e_g \approx \frac{4\pi\chi_l B_{\nu_l}(T)\alpha t_{pass}}{\rho}, \quad (45)$$

where we denoted $\alpha \equiv |\bar{J}/S - 1|$. In stellar atmospheres, the ionization energy is usually less, or of the same order, than the translational energy, while the excitation energy is negligible, so we can approximately assume $e_g = RT$ [erg/g] (μ is taken to be 1). By putting $\alpha = 0.5$ as a mean value in the region of interest, we can estimate the fraction of the gas energy emitted in one line as

$$\frac{\Delta e_g}{e_g} \approx 1.72 \cdot 10^5 \frac{B_{\nu_l}(T)}{v_g \rho \lambda \sqrt{T} A_m}, \quad (46)$$

where λ is in \AA . As can be seen, the ratio $\Delta e_g/e_g$ for a given species *does not depend on the line strength or chemical abun-*

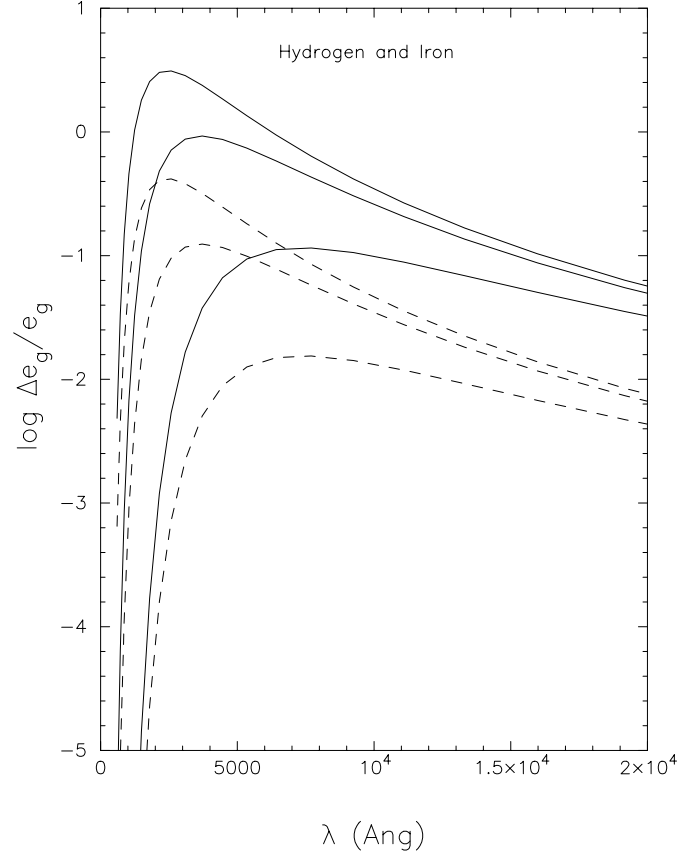


Fig. 8. Ratio $\Delta e_g/e_g$ for one hydrogen line (solid) and for one iron line (dashed) as function of λ for $\rho = 10^{-10} \text{ g cm}^{-3}$ and $T = 5000, 10000$ and 15000 K (from top to bottom, respectively). A $v_g = 10 \text{ km/s}$ value has been adopted

dance, but only on the wavelength, molecular weight, ρ , T and v_g . The curves $\Delta e_g/e_g$ for H and Fe lines are presented in Fig. 8 for $\rho = 10^{-10} \text{ g cm}^{-3}$, $T = 5000, 10, 000, 15, 000 \text{ K}$ and for $v_g = 10 \text{ km/s}$ (\approx sound velocity).

An important conclusion is that in the same spectral domain all lines contribute nearly equally to the total gas cooling, notwithstanding their strength and only weakly depending on the mass of the element. For example, at $T = 9000 \text{ K}$ Ly α contributes about 10 times less than each of thousands iron lines from the first packet in Fig. 2. We, however, should keep in mind that Eq. (46) only applies to the Doppler line profile.

In the $\lambda > 2000 \text{ \AA}$ domain, and for low postshock densities ($\rho \leq 10^{-10}$), as follows from Eq. (46), the ratios $\Delta e_g/e_g$ would be higher than shown in Fig. 8. In this case some strong lines of light elements, like Mg or Ca, can be dominant. Such low densities may occur in shocks propagating in the outer part of the stellar atmosphere, where the preshock density can be about $10^{-14} \text{ g cm}^{-3}$. For example, such conditions are typical for the late evolution of shocks in the RR Lyrae stars. However, very strong lines must be already blocked in the fine shock structure, where the conditions and cooling sources are essentially different from those assumed for the radiative wake (i.e. LTE, statistical equilibrium, radiative equilibrium in the Lyman con-

tinuum). If so, these lines cannot contribute effectively to the cooling of the radiative wake, but they can cool the gas in the fine structure. Indeed, the geometrical scale, corresponding to $\Delta\tau(\text{Mg II } 2797 \text{ \AA}) \approx 1$ is about $10^2 - 10^3$ cm, which, according to Narita (1973) and Fadeyev & Gillet (1998), is the typical scale of the thermalization zone ($T_e \neq T_a$). In most of this zone, the electron-atom elastic collision rate and collisional excitation rate can be large enough to provide a coupling with the main thermal pool of the gas (i.e. with heavy particles). So electron excitations and subsequent radiative de-excitations in strong lines, like the Mg II line, can provide a non-negligible cooling source. It thus seems important to include strong lines, like the Mg II or Ca II resonant lines, into the energy balance in the fine shock structure.

The difficulty of the evaluation of the thermal structure of the wake, however, is that the $\Delta\tau \approx 1$ zones, calculated for different lines, have different geometric extent, so a full statistical analysis of all lines is needed. Such an analysis will be presented in a forthcoming paper, but we give a preliminary discussion of this topic in the next section.

3.3.4. Heating zones

In Figs. 4, 5 and 6 one can see the heating effect ($\bar{J}/S > 1$), mentioned previously, appearing near the boundaries of the hot wake. More precisely, this heating takes place within the zones $\Delta\tau$ of about few units at both ends of the hot wake, in the regions with lower temperatures. Its physical origin can be demonstrated as follows. Under LTE, and if the wake is not very optically thin in the line, at τ_{s1} we have approximately $I^- \rightarrow B_\nu(T_w)$ and $I^+ \rightarrow B_\nu(T)$, which leads to

$$\frac{\bar{J}}{S} \approx \frac{B_\nu(T_w) + B_\nu(T)}{2B_\nu(T)} > 1, \quad (47)$$

and thus heating takes place. As the shock proceeds towards the surface, the wake becomes optically thin and $I^- \rightarrow 0$ at τ_{s1} . Consequently, \bar{J}/S diminishes (Fig. 6). At optical distances of about 5-10 behind the wake the heating ceases due to the approach to radiative equilibrium, which blocks photons.

The peak of \bar{J}/S in the preshock region is due to the absorption of the continuous radiation in the line, and thus depends in a complicated way on several parameters: optical width of the wake, line-to-continuum opacity ratio, velocity jump, absorption profile, slope of the unperturbed source function. For example, the heating in the preshock region would be negligible in the spectral domain where the wake is optically thin *in the continuum* and when the Doppler jump at the front is considerably larger than the line Doppler width. This follows from the fact that in the preshock co-frame (in which \bar{J}/S is to be evaluated), the intensity I^+ at the center of the absorption corresponds to the far wing of the postshock absorption, i.e. it is produced by zones located deeper than the hot wake, which have the unperturbed temperature. On the other hand, the heating rate per unit mass is enhanced due to lower density in the preshock region. It seems important to study this question in more detail.

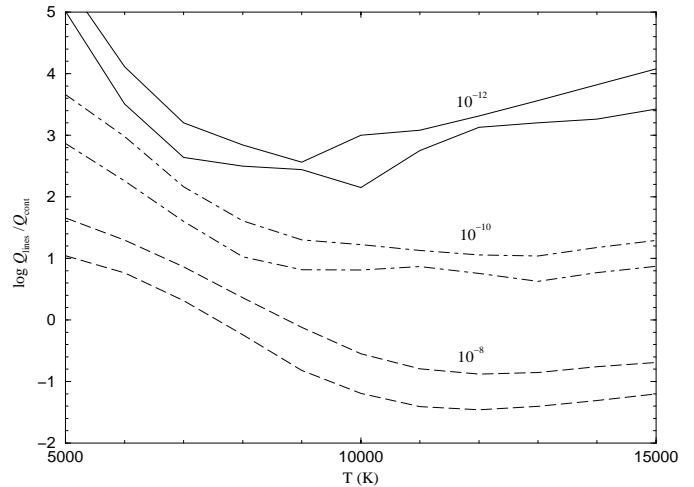


Fig. 9. Ratio of the cooling rates $Q_{\text{lines}}/Q_{\text{cont}}$ for three densities $\rho = 10^{-8}$, $\rho = 10^{-10}$, and $\rho = 10^{-12}$ g.cm $^{-3}$ (as indicated) and solar composition. The Lyman continuum is omitted from Q_{cont} . For Q_{lines} , lines with line core opacities greater than 10^{-5} cm $^{-1}$ (thin lines) or 10^{-4} cm $^{-1}$ (thick lines) are discarded

4. Radiative cooling in the whole spectrum

In the previous section we showed that the weak lines are very effective in cooling the shock wake. Now it is important to estimate how effective is the total line cooling with respect to the continuum. In other words, we wish to evaluate the ratio of the two terms on the right hand side of Eq. (10). This ratio must depend on the gas parameters, atomic concentrations, position in the wake, and transfer effects (b-b scattering, non-LTE, etc.). Because we cannot resolve this problem to its full extent, we consider here only the limiting case of optically thin gas under LTE. According to our previous results, such an approximation fully applies to the zone $\Delta\tau \leq 1$ behind the front of a shock in a dense atmosphere (where LTE is valid). We also assume $J_\nu \ll B_\nu(T)$ for the continuum radiation, $\bar{J}_l/S_l = 0.5$ and $S_l = B_\nu(T)$ for the lines. Finally, defining $Q_{\text{cont}} \equiv (De_g/Dt)_{\text{cont}}$ and $Q_{\text{lines}} \equiv (De_g/Dt)_{\text{lines}}$, the terms in (10) can be expressed through the Planck mean opacities: $Q_{\text{cont}} = k_{Pc}$ ($\approx \chi_R$), and $Q_{\text{lines}} = 0.5k_{Pl}$. To account for the fact that the strongest lines, as well as the Lyman continuum, do not contribute to cooling in the radiative wake because of their blocking, we eliminate from k_{Pl} all transitions whose line center opacity is greater than a given threshold and for which the front optical depth would be greater than 1. This excludes Lyman transitions, as well as H α , Mg II, Ca II, and some other prominent transitions. We thus probably underestimate Q_{lines} , while Q_{cont} is overestimated.

In Fig. 9 we trace the ratio $Q_{\text{lines}}/Q_{\text{cont}}$ as a function of T for three values of ρ : 10^{-8} , 10^{-10} and 10^{-12} g cm $^{-3}$.

As seen from the figure, even without Lyman and some other strong line transitions, the ratio $Q_{\text{lines}}/Q_{\text{cont}}$ can be important when the lines of heavy elements are included, especially at moderate temperatures or densities. Note that the present quantitative results refer to solar composition. For Population II stars,

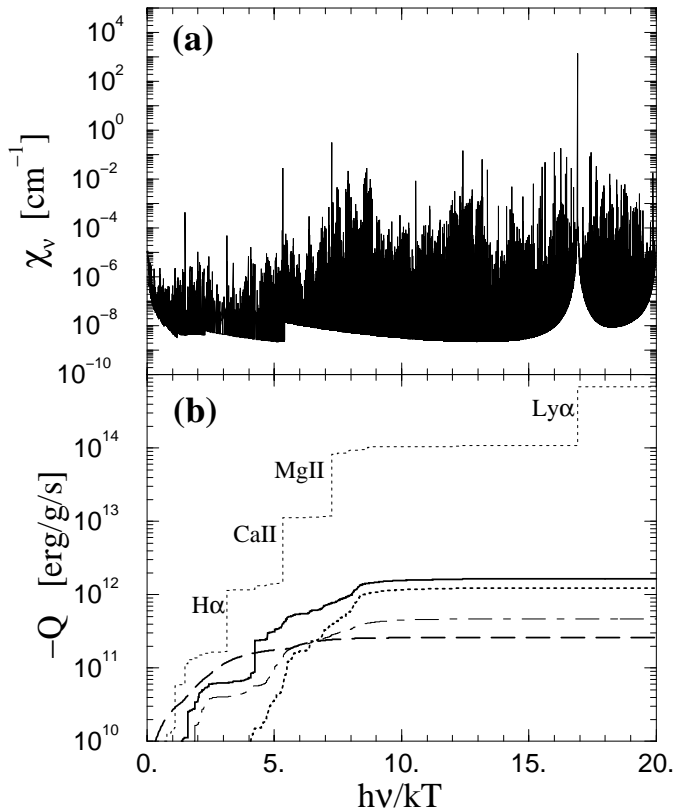


Fig. 10a and b. Contributions to the cooling rates in an optically thin case and under LTE for $T = 7000$ K and $\rho = 10^{-8} \text{ g cm}^3$, with solar abundances. **a** the monochromatic opacity; lines are Doppler broadened except for H lines. **b** the cooling rate Q when integrated starting from $h\nu/kT = 0$: for the continuum only without Lyman (thick dashed line), for all the lines with some major contributors indicated (dotted line), for lines with a line core opacity smaller than 10^{-5} cm^{-1} (dot-dashed line) or 10^{-4} cm^{-1} (thick solid line) and, in the latter case, the contribution of Fe lines (thick dotted line).

the expected ratio $Q_{\text{lines}}/Q_{\text{cont}}$ will be diminished proportionally to the element depletion.

With the increasing distance from the front, the approximation of an optically thin gas becomes no longer valid, because for a part of lines $\bar{J} \rightarrow S$. Consequently, the local ratio $Q_{\text{lines}}/Q_{\text{cont}}$ would decrease by an unknown factor, averaged over all lines.

To demonstrate the contribution of different lines to the cooling sum, in Fig. 10 we show the contributions of different elements to $\log Q_{\text{lines}}$ in the optically thin case over the whole spectrum, for typical values $T = 7000$ K and $\rho = 10^{-8} \text{ g cm}^{-3}$. Following the above reasoning about radiative equilibrium in the strongest lines, we excluded the lines which exceed the threshold opacity of $\chi_{\nu} = 10^{-5}$ or 10^{-4} cm^{-1} . We see that the strongest contribution to Q_{lines} belongs to the first Fe line packet, located at $h\nu/kT \approx 8$.

The important question of the temperature structure of the wake was not discussed in this first paper. In view of the present results, this structure should be calculated simultaneously with the local cooling rate, only starting from the shock front inward. Otherwise, if we try to evaluate the instant cooling rate at some

point of a given trial wake (in order to apply some structure-correction technique), we can easily be wrong. Indeed, if we take an initially optically thick wake, we shall find a negligible line cooling due to the initially large optical depth, and this result would confirm the wrong optically thick wake model. In the same way, we shall find a high cooling rate in an optically thin trial wake. However, in these cases, the information about line cooling *was already included* in the initial wake structure, so the result is not self-consistent.

Preliminary estimations of the radiative wake structure, with and without spectral lines, revealed that the effect of lines, especially iron lines, on the postshock cooling is dominant. Namely, due to the very strong cooling in the $\Delta\tau \leq 1$ region behind the front, the gas entering the postshock region cools much faster than in the continuum only, which substantially reduces the spatial dimension of the wake. The estimation of the true thermal structure of the shock wakes is especially important for interpretation and modelling of the shock-induced emission in the lines, for example in pulsating stars. We intend to perform such a detailed analysis of the radiative wake structure in the Paper II.

5. Conclusions

The radiative cooling of shock waves in dense stellar atmospheres is studied by means of the radiative transfer analysis for a line across a simplified shock model. The results allow us to make several important conclusions.

In the shock wake, at static optical distances (in the line core) from the front $\Delta\tau < 1$, independently of the optical width of the whole wake or of the depth of the front, the cooling in the lines is dominant over that in the continuum. The line cooling is found to be effective for postshock densities $\rho = 10^{-12} - 10^{-8} \text{ g cm}^{-3}$ and temperatures $T \leq 10^4$ K. We, however, suggest that strong lines, like Lyman or Mg II resonant lines, do not cool the gas because their photons are blocked in the fine shock structure. Also, strong but few lines contribute much less to the total cooling than weak but numerous lines, especially Fe I and Fe II lines. At larger optical distances from the front ($\Delta\tau > 5 - 10$) the radiative cooling occurs mainly through the H continua (Balmer and higher series).

Two regions of heating are found: one just before the front, first discussed by Mihalas (1969), due to the line absorption of the hot *continuous* radiation from the wake; and the second region just behind the radiative wake, due to absorption of the hot *line radiation* coming from the wake. Such a heating can in principle affect the thermal balance in the atmosphere of a pulsating star. For example, one can expect that due to this effect, the problem of the unphysical “supercooling”, detected earlier in some hydromodels with very strong shocks (e.g. Fokin 1992), can be eliminated.

Because the line cooling was found to increase with decreasing gas density, we may speculate that, as the shock propagates through a stellar atmosphere with decreasing ρ , the cooling rate in the wake increases. Consequently, its width would decrease. Eventually, the cooling becomes strongly line-dominated. To-

gether with the adiabatic cooling, this can lead to a very small optical width of the wake, so the emission can no longer be seen. This effect may explain the absence of the strong $H\alpha$ emission in some pulsating stars, like RR Lyrae, where shocks are very strong but form relatively high in the atmosphere.

Recently, Voitke et al. (1996) concluded that the most important contributors to the gas cooling in shocked atmospheres with $\rho \approx 10^{-10} \text{ g cm}^{-3}$ are the hydrogen continua, especially the Lyman continuum. However, considering their limitation to low-density stellar gas, we have some doubts about this result. Indeed, for typical conditions of normal and cool atmospheres (as δ Cephei, RR Lyrae or W Vir stars), the Lyman continuous radiation must be blocked already in the fine shock structure (at a distance $\approx 10^3 - 10^4 \text{ cm}$ from the front), so it can hardly cool the gas. This lets us suggest that the model of these authors is not very relevant for shocks in dense stellar atmospheres.

As a continuation of our study, in a forthcoming paper we shall examine the structure of the radiative shock wake with a more sophisticated analysis of the lines and continuum contributions to the gas cooling.

Acknowledgements. We thank F. Gonzalez for his help in operating with the spectral databases, and P. Voitke for fruitful discussions and remarks on this paper. We are also grateful to the anonymous referee for his valuable comments on the text. The work of ABF has been done in part under the auspice of the Ministère de l'Enseignement Supérieur et de la Recherche, France, in 1998.

References

- Castor J.I., 1972, ApJ 178, 779
 Cox D.P., Tucker W.H., 1969, ApJ 157, 1157
 Cunto W., Mendoza C., Ochsenbein F., Zeippen C.J., 1993, A&A 275, L5
 Fadeyev Yu., Gillet D., 1998, A&A 333, 687
 Fadeyev Yu., Gillet D., 2000, A&A 354, 349
 Fokin A.B., 1992, MNRAS 256, 26
 Gillet D., 1999, In: Brun R., et al. (eds.) 21st International Symp. on Rarefied Gas Dynamics. Marseille, July 1998, Vol. II, p. 517
 Gillet D., Lafon J.P.J., David P., 1989, A&A 220, 185
 Hill S.J., 1972, ApJ 178, 793
 Huguet E., Lafon J.P.J., 1997, A&A 324, 1046
 Klein R.I., Stein R.F., Kalkofen W., 1976, ApJ 205, 499
 Klein R.I., Stein R.F., Kalkofen W., 1978, ApJ 220, 1024
 McWhirter R.W.P., Thonemann P.C., Wilson R., 1975, A&A 40, 63
 Mihalas D., 1969, ApJ 157, 1363
 Mihalas D., 1978, Stellar atmospheres. San Francisco
 Narita S., 1973, Progr. Theor. Phys. 49, 1911
 Praderie F., 1981, Activity and outer atmospheres of the stars. Lect. at the 11th Advanced Course of the Swiss Soc. of Astrophys. and Astron., Saas-Fee
 Seaton M.J., 1987, J. Phys. B: At. Mol. Opt. Phys. 20, 6363
 Skalafuris A.J., 1965, ApJ 142, 351
 Skalafuris A.J., 1968, Ap&SS 2, 258
 Whitney C.A., Skalafuris A.J., 1963, ApJ 138, 200
 Voitke P., Krüger D., Sedlmayr E., 1996, A&A 311, 927
 Zel'dovitch Ya.B., Raizer Yu.P., 1966, Physics of shock waves and high-temperature hydrodynamic phenomena. Academic Press, New-York